16TH EUROPEAN CONFERENCE ON EARTHQUAKE ENGINEERING THESSALONIKI 18 - 21 JUNE 2018

OPTIMIZED DESIGN AND MOMENT-CURVATURE DIAGRAM CONSTRUCTION FOR BIAXIALLY LOADED ELEMENTS

Igor GJORGJIEV[1], Borjan PETRESKI[2]

ABSTRACT

The combined action of biaxial bending and axial load is very common among the reinforced concrete vertical elements, especially in the seismic prone areas and most frequently authoritative for their assessment and design. The most commonly used procedure for design is a trial method where the amount of rebar is assumed in the beginning and the capacity ratio is calculated. The Eurocode-2 provision, in the absence of an accurate cross section design for biaxial bending, offers simplified criterion that ignores the interaction between the both principal moments. It involves using the 'load contour method' by Bresler which is approximate and unsafe for the design of rectangular, circular or elliptical columns. Thus, the interaction diagrams and approximation curves used for reinforced concrete sections design do not have the ability to offer an adequate procedure for the design of irregular shaped cross sections.

In this study particularly, the influence of compatible section mesh and integration techniques on the numerical solution of the equilibrium equations of various regular and irregular reinforced concrete sections under biaxial bending and axial force is presented. The calculations were processed by software created by the first author. It is concluded that the mesh optimization is playing a great role in the accuracy and computational efficiency of the solution. Therefore, the coarser meshing provides excellent results within regular cross-sections while the finer mesh in combination with Gaussian quadrature integration is optimal for the design and calculation of M-N capacity and ductility of irregular and complex cross-sections.

Keywords: reinforced concrete; biaxial loading; meshing; optimized design; moment-curvature;

1. INTRODUCTION

Due to initial geometrical imperfections, as well as misalignment of the active loads, the compression members in structures are subjected to moments in addition to axial loads. The eccentric axial loading of the columns is usually represented through sideways earthquake and wind loading or a portion of unbalanced moments at the ends of the beams supported by the vertical load bearing components of the structure. The combined action of biaxial bending and axial load is very common among the reinforced concrete vertical elements and most frequently authoritative for their assessment and design.

Even though much consideration about the analytical representation of this phenomenon is given in a large amount of previous studies, very few authors reflect on the particular problem of design of sections subjected to biaxial bending in addition to the axial force. Consequently, the codes of practice

[1]Assoc. Prof. PhD, Institute of Earthquake Engineering and Engineering Seismology, University "Ss. Cyril and Methodius", Skopje, Republic of Macedonia, igorg@pluto.iziis.ukim.edu.mk

[2]Ass. MSc, Institute of Earthquake Engineering and Engineering Seismology, University "Ss. Cyril and Methodius", Skopje, Republic of Macedonia, borjan@pluto.iziis.ukim.edu.mk

In line with the A/RES/47/225 resolution of the United Nations, the provisional State name is *former Yugoslav Republic of Macedonia (F.Y.R.O.M.)*. Alternative names reflect the views of the Authors and are not adopted by the Hellenic Association of Earthquake Engineering.

do not directly give specific method for designing of the biaxially bent elements, instead directing at solutions following basic principles and design charts.

Earlier research has generally had the focus on different analytical and numerical methods for determining of the most accurate and efficient algorithms to compute the interaction surfaces for sections of arbitrary shape. Sfakianakis (2002) proposed a new method based on the fiber model concept and pixel originated computer graphics in order to study reinforced concrete sections of various shapes and contours subjected to biaxial bending. Bonet et al. (2006) have demonstrated that the integration methods based on the Gauss-Legendre quadrature turn out to be very effective for computation of the M-N interaction diagrams. More recently, Papanikolau (2012) in his analysis of arbitrary sections in biaxial bending and axial load additionally implements a moment-curvature response analysis of the reinforced concrete and composite sections. Essentially, these studies provide important features within the research domain while also influencing further developments in the fields of structural design, assessment and optimization.

Such development is contained in the work presented through improvement in the meshing and the calculation algorithm and this issue is flattened for application in the common design engineering environment. Benefitting sophisticated meshing and two separate stress integration procedures along with the updatable material behavior relationships the capacity of the cross-section is obtained. It is then advanced to determine the exact reinforcement required for an arbitrary reinforced concrete cross-section to withstand the predefined external forces (biaxial bending moments and axial forces) acting on it. For that purpose, an innovative design and very effective root-finding algorithm is implemented in the program package written in C++ and C#. Through an example, the developed algorithm is tested on a representative cross section. It is then observed that the design of a reinforced concrete section can be optimized with regarding to the speed without losing the accuracy of the solution.

2. MATERIAL PROPERTIES

The current version of the software presented in this paper is adapted to comply with the latest Eurocode 2 draft making it operational in the countries practicing the European codes and for researchers making comparative studies with those regulations. However, using the modular programming technique that separates the functionality of the program into independent modules for the development of the software, this feature is easily adaptable for upgrade.

Regarding the materials comprising the cross-sections under investigation, Eurocode 2 definitions of the stress-strain relationship of the concrete and steel are used. Along with the aforementioned assumptions, the stress-strain graphical representations of the materials are the basic theoretical background and limitations to this newly developed computational tool.

2.1 Concrete

The stress-strain relationship of the concrete in the current version is parabolic-rectangular curve, as shown in Figure 1 below. Nevertheless, it also supports other simplified stress-strain diagrams for characterization of the concrete material, such as high-strength concretes and confined concrete, as well. This attribute results from the adaptable modular modification of the stress-strain relationship depicted in improvement of the strength and the critical strains.

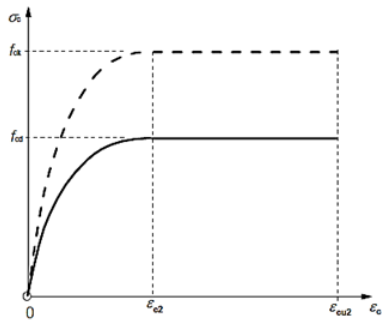

$$\sigma_c = f_{cd}\left[1-\left(1-\frac{\varepsilon_c}{\varepsilon_{c2}}\right)^n\right] \quad \text{for} \quad 0 \le \varepsilon_c \le \varepsilon_{c2}$$

$$\sigma_c = f_{cd} \quad \text{for} \quad \varepsilon_{c2} \le \varepsilon_c \le \varepsilon_{cu2}$$

Figure 1. Parabola-rectangle stress-strain diagram for concrete, EN 1992-1-1 (2004)

The values of the parameters in this figure are specified within Table 3.1 from EN 1992-1-1 (2004). The parameter f_{cd} is the design compressive strength (f_{ck}/γ_c, where γ_c is the partial safety factor for concrete prescribed in Clause 2.4.2.4, Table 2.1N) which in combination with the design tensile strength f_{ctd} is given in Clause 3.1.6 of EN 1992-1-1. It is important to note here that this version supports the application of confinement of the concrete as well.

2.2 Reinforcing steel

Theoretically, the behavior of the reinforcing steel material is represented through an elasto-plastic stress-strain relationship curve. Its constituent parts include a linear elastic region, yielding phenomenon resulting in perfectly plastic behavior and strain hardening to further and maximum deformation. However, the Eurocode 2 assumes simplified material diagrams for the need of practical application and proposes elastic-perfectly plastic constitutive law for the reinforcing steel defined by a bilinear diagram (Figure 2). That simplified stress-strain diagram required for cross-sectional design is applied in the software presented. Its characteristic parameters such as the yield strength – f_{yk}, the design strength – f_{yd}, the partial safety factor for steel – γ_s, the typical strain values of ε_{ud} and ε_{uk} (where ε_{uk} is the characteristic strain of reinforcement at maximum load and the recommended value for ε_{ud} is $0.9\varepsilon_{uk}$) and the design value of the modulus of elasticity – E_s are indicated in Chapter 3.2 of EN 1992-1-1.

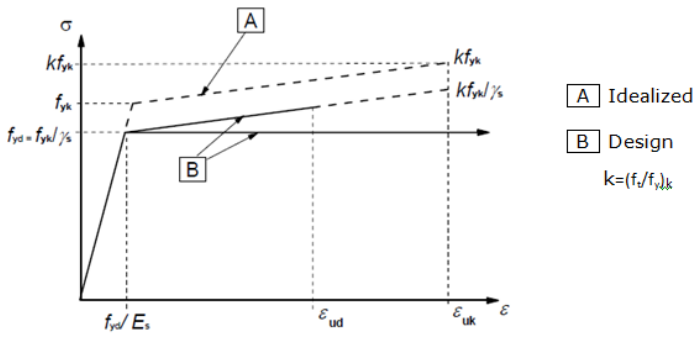

Figure 2. Idealized and design stress-strain diagrams for reinforcing steel, EN 1992-1-1 (2004)

3. GEOMETRIC TRANSFORMATION

The choice of the origin of the local reference system is initiation of the cross-sectional analysis of structural elements. The geometric centroid is the center of a cross-section without regard to the material properties of its components. It is assumed as the point where the external forces act on the cross-section. The plastic centroid, on the other hand, can be calculated by applying force equilibrium conditions to the stresses in various cross-sectional components. When discussing about a complex multi-material section such as the reinforced concrete, the plasticity is dependent on the both

materials. The coordinate location of the plastic centroid of the cross section is calculated by Equations 1 and 2, where *x, y, x'* and *y'* are the distances of the reinforcement bars to the edge of the cross-section.

$$x_{PC} = \frac{\alpha_{cc} f_c' bh^2 / 2 + A_s f_y x + A_s' f_y x'}{\alpha_{cc} f_c' bh + A_s f_y + A_s' f_y} \tag{1}$$

$$y_{PC} = \frac{\alpha_{cc} f_c' b^2 h / 2 + A_s f_y y + A_s' f_y y'}{\alpha_{cc} f_c' bh + A_s f_y + A_s' f_y} \tag{2}$$

In the case of regular symmetric polygonal cross-sections with uniform distribution of the reinforcement steel along the element contours, the geometric and the plastic centroids match. However, for unsymmetrically reinforced concrete sections or sections of irregular shape (L, T, U etc.) where the both centroids differ, the load must pass through the plastic centroid. Then, the calculation of eccentricity of the applied biaxial moments is quite straightforward measured with respect to the plastic centroid. With the purpose of compatibility of the local reference system, translation of coordinates is hereby introduced.

Then, in order to transform the initial coordinates of the cross section to the origin of the geometric or plastic centroid a complex transformation is performed. It is implemented by combining of two basic transformations – translation and rotation. In order to represent all transformations in the same form as the rotations, it is approached to application of homogeneous coordinates, which make the representation more consistent and easier to use. The homogeneous coordinates add an extra virtual dimension whose value is 1, which for instance allows representation of translations as matrix multiplication instead of vector addition. Finally, the combination of the T (translational) and R (rotational) matrices is a homogeneous transformation matrix denoted as C. It is very important to note here that the matrix C represents a rotation followed by translation and reversing the cases most often does not work. The resulting matrix C is shown in Equation 3.

$$C = \begin{bmatrix} c & s & 0 \\ -s & c & 0 \\ 0 & 0 & 1 \end{bmatrix} \begin{bmatrix} x_t \\ y_t \\ 1 \end{bmatrix} = \begin{bmatrix} c & s & x_t \\ -s & c & y_t \\ 0 & 0 & 1 \end{bmatrix} \tag{3}$$

4. MESH AND INTEGRATION

4.1 Mesh generation

In order to solve the two-dimensional problems analytically, a discretization and integration procedure over the finite-discrete domain is required. The cross-sectional analysis of reinforced concrete structures demands optimized meshing discretization of the infinite continuum and accordingly adjusted integration methods for substantial computational efficiency due to its multi-material nature. Therefore, a guaranteed-quality two-dimensional mesh generating technique is applied and the infinite continuum is discretized by the mean of Ruppert's Delaunay refinement algorithm, Shewchuk (2002). The triangulation method includes user-specified constraints on angles and triangle areas, user-specified holes and concavities, and economical use of exact arithmetic to improve robustness.

The triangulation, depending on the complexity of the domain, is constructed between the vertices and the segments, which can be defined by the section geometry or by subdivision and creation of good-quality finer mesh triangles, Figure 3. The coarser triangulation (left) is called a constrained Delaunay triangulation (CDT) where each segment is depicted as a single edge. On the other hand, the finer

mesh (right) is labelled as a constrained conforming Delaunay triangulation (CCDT) and it is the optimized meshing concept for achieving excellent accuracy solution.

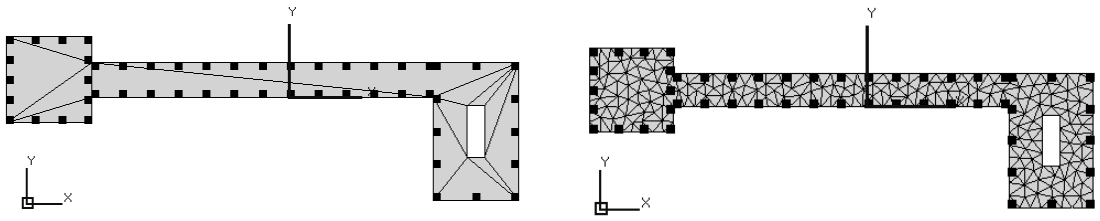

Figure 3. CDT and CCDT triangulation

The section under consideration is constructed from collections of lines (segments) and vertices which generate planar straight line graphs. Each of the graphs is denoted as a single region and the combination of the regions represents the actual geometry of the cross-section with all of its constituent material and shape variations. The external borders of the cross-section are all parts of outer regions while the holes and the concavities are subtracted from the total area using inner regions. The unsymmetrical section in Figure 3, for instance, is composed of 3 outer regions and the hole is characterized by 1 inner region. Pure representation of the different regions of the cross-section is observable within the CDT triangulation (left) where each segment of the region symbolizes a single edge of the triangular mesh.

4.2 Stress integration

Subsequently, as an accurate and most suitable meshing preference of the cross-section is determined and the material properties are pre-defined through the stress-strain diagrams, the integration over the cross-sectional area is the issue to be tackled. Assuming that the strain distribution across the section is defined and the stress is defined in terms of the strain, one can obtain the strain and stress as a function of the location of the integration area with accordance to the neutral axis. The required axial – flexural stress resultants for a particular strain distribution corresponding to Figure 4 are shown in Equations 4, 5 and 6.

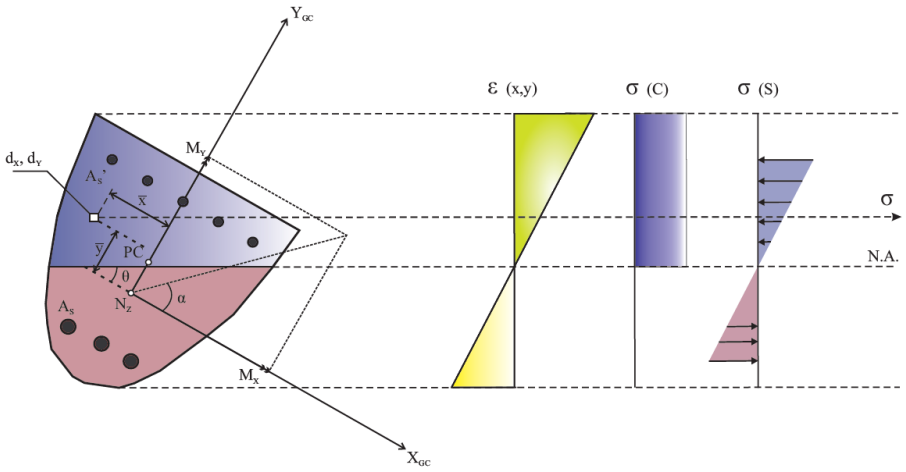

Figure 4. Stress and strain diagrams of a cross-section subjected to bending about an arbitrary axis

$$N_z = \int_x \int_y \sigma(x, y) dx dy \tag{4}$$

$$M_x = \int_x \int_y \sigma(x, y) dxdy \cdot \bar{y} \tag{5}$$

$$M_y = \int_x \int_y \sigma(x, y) dxdy \cdot \bar{x} \tag{6}$$

There are several integration practices in the literature applied very frequently in the analysis of two-dimensional problems. Within the study presented and the current software development, two integration procedures are preserved. Depending on the complexity of the mesh and the irregularity of the cross-section, different integration method suits particular triangulation differently. For example, the coarser meshing employing simpler triangles that use the cross-sectional edges as element edges, requires minimal computational and mathematical complexity for resulting in sufficiently accurate solution. The implementation of the simple trapezoidal rule for approximating the definite integral is consequent but its application is limited and recommended for the CDT meshing and regular cross-sections (including I, L, T sections that can be simplified with as few triangles as possible; the circular section, on the other hand requires many triangles to represent its circumference approximately accurate). Furthermore, Gaussian quadrature is the additional integration procedure supported in this analytical software tool. This particular method is especially required for establishing accurate solution for more complex meshes. For the need of conforming to the most complex challenges in the applicative field such as design of irregular cross-sections and reducing of the possible errors, the software supports Gaussian quadrature to an order of 3 to 16 Gauss points per triangle element.

5. FAILURE SURFACE

The construction of the failure surface for a chosen section depends on the cross section shape, the amount of the steel reinforcement, its particular distribution across the section and a certain strain state. Then, by integration of two essential boundary condition equations, the plane failure surface with the ultimate bending moment and axial force capacity can be constructed. Repeating the integration for a chosen finite number of strain conditions, in order for the description of the entire section capacity, from pure axial compression to pure axial tension, the limit values of the corresponding bending moments and axial forces are obtained, whose graphical representation is the diagram of interaction M–N. The possible regions of concrete and steel strain diagrams distribution at varying cross-sectional failure points are defined via the following regions:

- Region 1 – incorporates the circumstances where the section failure is controlled by steel breaking. It is defined by setting a constant strain limit in the reinforcement and a variable concrete strain state. The failure occurs because of exceedance of the bearing capacity of the reinforcement steel.

ε_S = -25 ‰ = constant
ε_C = -25 ‰ ÷ 3.5 ‰

- Region 2 – encompasses the cases in bending with or without compressive axial force within the relatively big or medium eccentricities. The failure occurs in the concrete part of the section while at the same time the steel reinforcement has or has not reached the yielding point. The result is a brittle failure.

ε_S = -25 ‰ ÷ 0 ‰
ε_C = 3.5 ‰ = constant

- Region 3 – characterizes the cases when the whole section is compressed (eccentric compression in the small eccentricity zone or a centric compression). The failure occurs when the limit strain of the concrete is reached.

ε_S = 0.0 ‰ ÷ 2 ‰ = constant
ε_C = 2 ‰ ÷ 3.5 ‰

Applying the above procedure, the ultimate capacity of a reinforced concrete section subjected to biaxial bending and axial force is obtained. However, unlike the interaction diagrams in the case of uniaxial bending, the biaxial bending diagrams normally demand spatial representation which substantially increases their practical application. Thus, by evaluating the interaction diagrams at various angles of the neutral axis, a series of diagrams is created to form the interaction surface, see Figure 5. Each point on this surface represents one particular set of axial load and bending about the major axes, x and y. It is generated using equators obtained as M_x - M_y interaction curves for varying levels of axial force, meridians matching different bending angles $\alpha = \tan^{-1} (M_x/M_y)$ or meridians relating to the neutral axis angle $\theta \neq \alpha$.

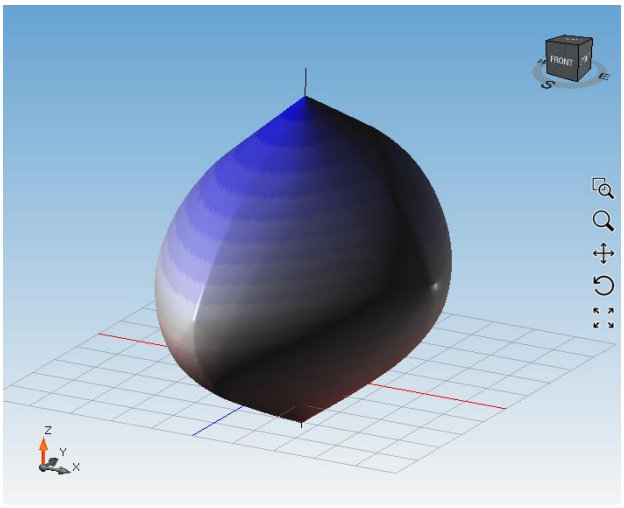

Figure 5. 3D failure surface of a rectangular section constructed with the software

6. DESIGN PROCEDURE ALGORITHM

The procedure for solution of the main reinforcement design issue while considering the arbitrary reinforced concrete sections is consisting of two interconnected iteration processes and fast-solving numerical algorithm called - the secant method. In the software build-up, two efficient iteration techniques are employed in order to approach and define the exact value of reinforcement needed for a pre-defined external actions. The first iteration is applied to determine the angle between the neutral axis of the section and x-x axis, named as θ. For the initial iteration an angle value of θ=0° is assumed meaning the neutral axis and x-x axis are compatible. Knowing the section geometry, the reinforcement distribution and the external loads, the first position of the cross-section neutral axis results in a certain amount of reinforcement and an initial amount of internal forces. In parallel, the position (depth) of the neutral axis relative to the outermost fiber of the section, d, is assumed and iterated in order to obtain the solution. By keeping the θ constant and iterating the depth of the neutral axis it is approached to acquiring a value close to the external axial load. After one of the parameters is determined, the angle is continuously iterated until the required reinforcement is sufficient to withstand the external biaxial moments. For a fast converging solution and efficient computation of the two iteration procedures, a root-finding algorithm that uses succession of roots of secant lines to better approximate a root of a function is used. Namely, the secant method shown in Figure 6, regarded as a finite difference approximation of Newton's method is applied and the exact design of the arbitrary cross-sections is performed.

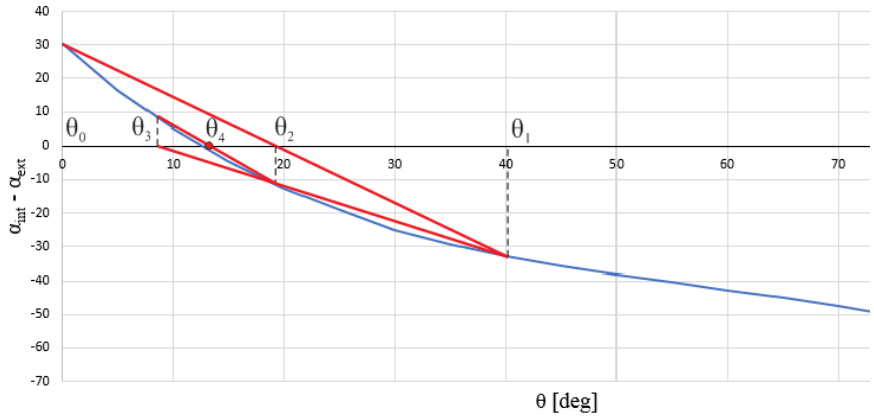

Figure 6. Secant method example for estimation of the angle of neutral axis

7. MOMENT-CURVATURE CALCULATION IN 3D

The moment-curvature relationships of a section are highly important in order to assess the ductility of the element, the amount of the possible redistribution of stresses and its resistance against dynamic loading. Even though, the yield curvature of the section is quite straightforwardly obtained from the strain profiles and the yielding of the longitudinal reinforcement, it is very important to obtain correctly the ultimate limit state from the ultimate strain profiles in the 3D domain. Considering the ultimate limit state of the section, it is defined as the failure strain when any of the components comprising the section reaches its own ultimate state. Whether it is the ultimate compressive strain of the concrete, the ultimate compressive strain when the whole section is under compression or the ultimate tensile strain in the reinforcement.

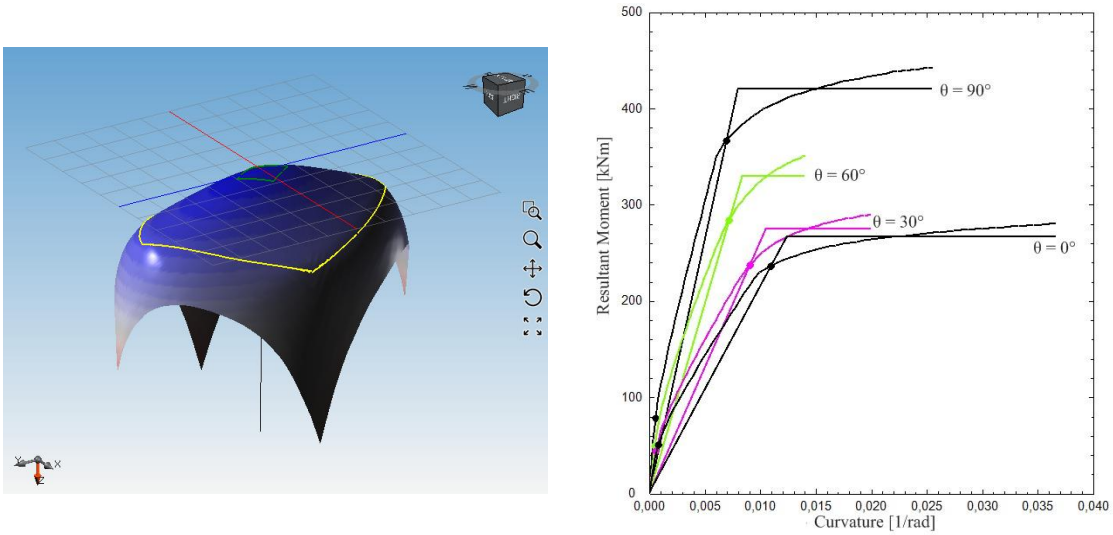

Figure 7. 3D and 2D moment-curvature representation of a rectangular section constructed with the software

When observing Figure 7, it can be inferred that the 3D moment-curvature diagram demonstrates great differences in the ductility of the cross-section at various angles of the neutral axis. Namely, the M-φ surface exhibits peaks in the capacity when the neutral axis position corresponds with the main orthogonal axes (x and y) of the rectangular cross-section or at angles of 0° and 90°. The yellow line on the surface denotes the yielding curvature at every neutral axis angle and it aids easier graphical evaluation of the ductility of the cross-section. It is therefore evident that the section behaves excellently ductile when considering the uniaxial response in one of the main orthogonal axes.

However, when the effect of the biaxial bending is taken into account, meaning the resultant direction of the both principal capacity moments is considered, the ductility of the cross-section clearly becomes an issue. Even though the section investigated shows reasonable ductility in the direction of the main axes, the occurrence of biaxial bending reduces its capacity regarding both the strength and the ductility. And for the case of biaxial bending, the loading resultant vector regularly influences the section under a certain angle between its axes of symmetry. Furthermore, the moment-curvature response of cross-sections of irregular shape adds up to the complexity of the calculation.

8. INFLUENCE OF MESH SIZE AND INTEGRATION METHOD ON RESULT

In order to analyze the influence of mesh size and integration method on the result, a representative regular cross-section is created (Figure 8, left). The analyzed section is rectangular with width of 40 cm and height of 60 cm. The reinforcement distribution is symmetrical with 25% of total rebar area per each side with a cover distance of 4 cm. In order to simulate a continuum, the 10 reinforcement bars are placed along each edge.

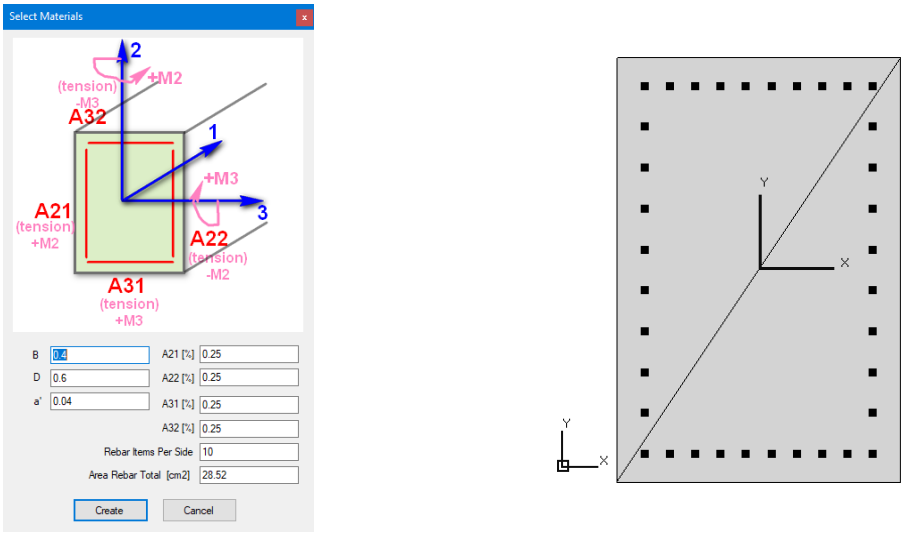

Figure 8. The analyzed cross-section data (left) and CDT mesh discretization (right)

The analyses are performed on the discretized section using two types of triangular meshes. Both the CDT (Figure 8, right) and the CCDT (Figure 9) mesh types are applied to the cross-section and their performance is subsequently examined. In the case of CCDT mesh four element sizes with maximum triangle area of 0.008, 0.004, 0.002 and 0.001 m^2 are analyzed.

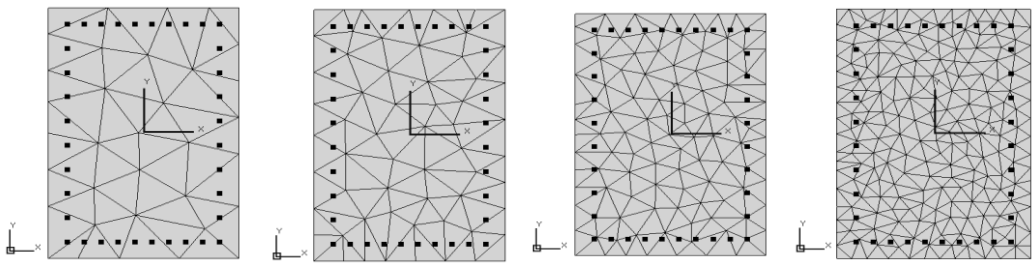

Figure 9. CCDT mesh discretization with maximum element area of 0.008, 0.004, 0.002 and 0.001 m^2

The calculation speed and solution error are analyzed in particular with both CDT and CCDT mesh types applied. The solution for this load case regarding the total reinforcement area and angle of the

neutral axis of the section, presented in Table 1, is 28.52 cm^2 and 30° (0.52360 rad) respectively.

Table 1. External loading values and solution parameters.

N [kN]	Mx [kNm]	My [kNm]	α [rad]	θ [rad]	Aa [cm2]	ε_S	ε_C
-508.55	188.15	265.88	0.95494	0.52360	28.52	0.0053	-0.0035

Regarding the CCDT mesh, two separate discretization techniques with varying maximum triangle element areas of 0.004 and 0.0005 m^2 are applied. For CDT meshing the trapezoidal integration method is used in order to calculate the internal compression force in the cross-section. The compression region has been divided in 50 equal height segments. In the case of CCDT the Gauss quadrature with seven integration points is used. Each of the three sections is analyzed three times and the calculation time and error are presented in Table 2. The calculation of the section analyzed with CCDT mesh and maximum element size 0.004 m^2 is 3.4 times faster than CDT mesh and 38 times more accurate. The errors obtained for each method of computing the design reinforcement area are presented relatively with respect to the solution parameters as prescribed in Equation 9:

$$Error(\%) = \left| \frac{Aa_i - Aa_{sol}}{Aa_{sol}} \right| \cdot 100 \tag{9}$$

where Aa_i is the value obtained for the *i*th-case for reinforcement area required and Aa_{sol} is the exact value of design reinforcement area obtained from the analytical solution. The most accurate solution is obtained with the CCDT technique and maximum element size of 0.0005 m^2 but the calculation time is slowest. Briefly, from the results obtained out of these analyses, it can be concluded that the optimal section mesh for cross-sectional analysis is CCDT with maximum element size of 0.004 m^2.

Table 2. Comparison of calculation time and error.

Mesh type	Integration points/ Segments	Maximum element area [m^2]	Average calculation time [sec]	Error [%] – θ iterated	Error [%] – θ = 30°
CDT	-/50	-	0.206	0.150	0.133
CCDT	7/-	0.004	0.060	0.042	0.0035
CCDT	7/-	0.0005	0.441	0.035	0.000

In order to compare the relationship between the solution error and the integration techniques, the results of the computational operations are presented in the following charts. The first comparison is performed for a predefined section rotation of 30° which correlates with the analytical solution. On the graph in Figure 10 the relationship between solution error and the number of Gauss integration points for all element sizes of the CCDT mesh is shown. Alternatively, the graph in Figure 11 presents the dependence of the error on integration segments used in CDT discretization. Hence, it can be concluded that the accuracy of the solution increases as the number of integration points and integration segments increases. It is a general case for all meshes implemented and investigated.

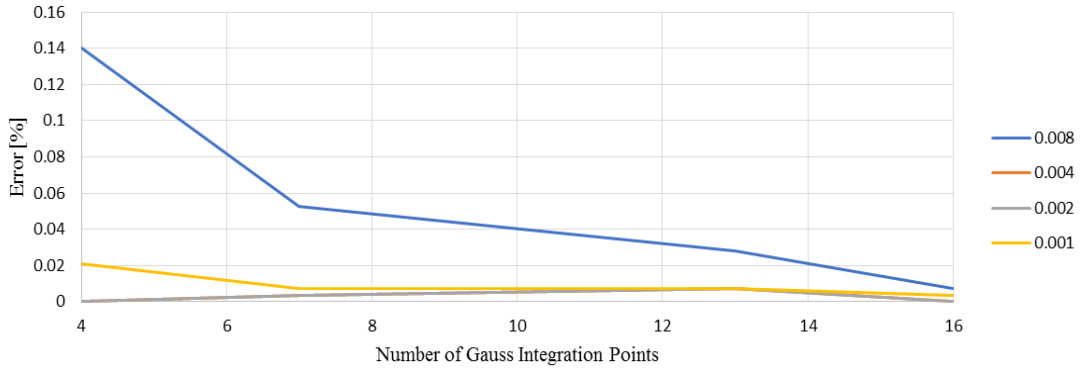

Figure 10. Dependence of error on number of Gauss integration points for predefined section rotation of 30°

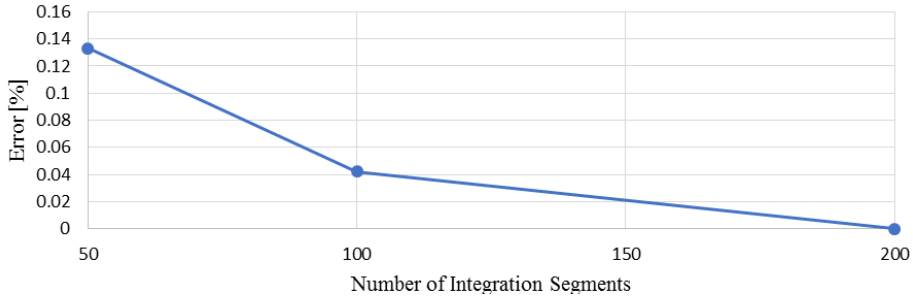

Figure 11. Dependence of error on number of integration segments for predefined section rotation of 30°

Finally, the influence of coarseness of the mesh on the solution is investigated on a section discretized by varying maximum triangle element areas of 0.001, 0.002, 0.004 and 0.008 m^2. The results are grouped by the number of Gauss integration points, shown in Figure 12. From the results obtained, it can be seen that decreasing the maximum element area from 0.008 to 0.004 m^2 dramatically increases the accuracy of the solution for cases with four and seven integration points. For higher order of integration points the difference in element size does not significantly influence the solution.

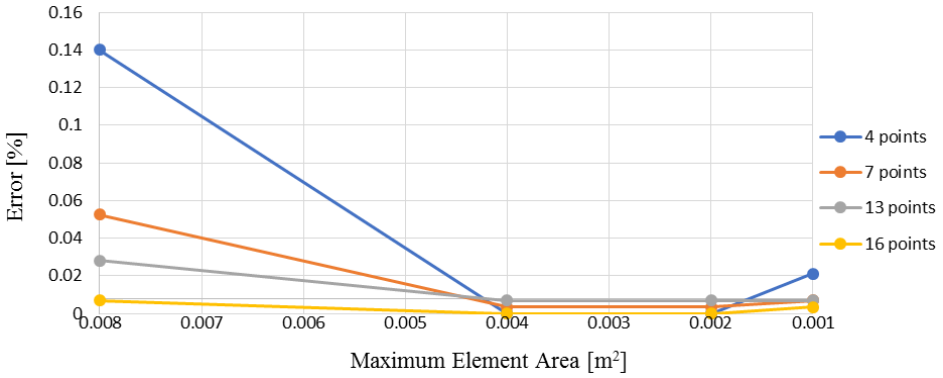

Figure 12. Dependence of error on element area for predefined section rotation of 30° (only CCDT mesh)

9. CONCLUSIONS

A new methodology was presented in this study for an optimized design and calculation of M-N capacity and ductility of arbitrary cross-sections subjected to axial load and biaxial bending. The method presented makes use of optimization in the meshing and implementation of two separate stress integration procedures depending on the complexity of the cross-section. The accuracy of the results is very high with regards to all types of sections investigated, with and without holes, composite or both

regular and irregular reinforced concrete types.

From the comparisons presented in Section 8, it can be established that with proper selection of the mesh type and integration method the design procedure for reinforced concrete members can be optimized regarding speed and accuracy. This approach can be implemented for predefined column shapes such as rectangular, T, L, I etc. The optimization of the calculation speed is very important for the design of large structures exposed to large number of load combinations. The performed analysis showed that the presented tool has large number of optimization parameters which are decreasing the calculation time without influencing the solution accuracy.

Finally, it can be stated that many advancements in the current software package are possible and investigated in the direction of transferring the solution from local cross-sectional, to a wider domain on a level of a full element and even a whole structure. Also, some other structural materials and elements are being considered for the future versions of the application such as pre-stressing tendons, jacketed cross-sections etc.

7. REFERENCES

Beyer, K., Dazio, A. & Priestley, M. (2008). Quasi-static cyclic tests of two U-shaped reinforced concrete walls. *Journal of Earthquake Engineering*, 12(7): 1023-1053.

Bonet, J., Barros, M. & Romero, M. (2006). Comparative study of analytical and numerical algorithms for designing reinforced concrete sections under biaxial bending. *Computers & Structures*, 84(31): 2184-2193.

CEN [European Committee for Standardization] (2004). Eurocode 2: Design of concrete structures – Part 1-1: General Rules and Rules for Buildings (EN 1992-1-1), Brussels.

CEN [European Committee for Standardization] (2003). Eurocode 8: Design of Structures for Earthquake Resistance, Part 1: General Rules, Seismic Actions and Rules for Buildings (EN 1998-1), Brussels.

Di Ludovico, M., Lignola, G. P., Prota, A., & Cosenza, E. (2010). Nonlinear analysis of cross sections under axial load and biaxial bending. *ACI Structural Journal*, 107(4), 390.

Sousa, J. B. M. & Muniz, C. F. (2007). Analytical integration of cross section properties for numerical analysis of reinforced concrete, steel and composite frames. *Engineering Structures*, 29(4): 618-625.

Sfakianakis, M. (2002). Biaxial bending with axial force of reinforced, composite and repaired concrete sections of arbitrary shape by fiber model and computer graphics. *Advances in Engineering Software*, 33(4): 227-242.

Papanikolaou, V. K. (2012). Analysis of arbitrary composite sections in biaxial bending and axial load. *Computers & Structures*, 98-99: 33-54.

Shewchuk, J. R. (1996). Triangle: Engineering a 2D quality mesh generator and Delaunay triangulator. In: Applied computational geometry towards geometric engineering, Springer Berlin Heidelberg, pp 203-222.

Shewchuk, J. R. (2002). Delaunay refinement algorithms for triangular mesh generation. *Computational geometry*, 22(1): 21-74.